MAPPING, DETECTION AND HANDLING OF SINGULARITIES FOR KINEMATICALLY REDUNDANT SERIAL MANIPULATORS

Zsolt KEMÉNY

Department of Control Engineering and Information Technology
Budapest University of Technology and Economics
H–1117 Budapest, Magyar Tudósok körútja 2, Hungary
Tel: 36 1 274 4435
e-mail: galaxy@impulzus.sch.bme.hu

Abstract

This paper deals with the singularities of kinematically redundant manipulators in terms of determining the singularity manifolds in configuration space, and detecting/handling singular configurations in a local kinematic planning environment. Using the example of a specific manipulator with 8 degrees of freedom, a systematic method is presented which is generally applicable to the given class of redundant arms. As a part of the method's principle, the effects of kinematic redundancy on the singularity manifolds are also addressed and explained. Finally, a local motion planning setup is shown where redundancy resolution can be used for singularity avoidance and handling strategies.

Keywords: differential kinematics, kinematic redundancy, singularity manifolds, singularity detection, singularity handling, parameterization through null space.

1. Introduction

Encountering a singularity implies the exhaustion of the manipulator's task space motion reserve in at least one dimension. This issue has received much attention throughout the entire history of robot motion planning and control, since singular configurations restrict the motion capabilities of the robot and cause numerical difficulties for the motion planner.

Research concerning singularities can be subdivided into three major topics. The determination of singularity manifolds for a given manipulator (in an *a priori* manner) relies largely on a symbolic differential kinematic description of the manipulator and usually defines the singularity manifolds with a *first order logical statement*. This a priori information can be used for global planning (the singularity manifolds being virtual obstacles in configuration space), local planning, especially for redundant manipulators (with virtual forces repelling the robot from singularities), and last but not least, construction of the manipulator, especially for cases where large singularity-free areas of operation have to be guaranteed (e. g. medical robots). The remaining two topics, namely on-line singularity detection and singularity handling usually go hand-in-hand, both applied as a *symptomatic treatment*, e. g. when a given singularity cannot be avoided. On-line singularity

detection can be performed upon computing the robot's current differential kinematic model, by examining the manipulator's Jacobian matrix. Is the proximity of a singular configuration detected, a singularity handling method can be used which ensures acceptable joint space velocities at the cost of locally deteriorating workspace motion.

Some singularities of redundant robots differ from those of non-redundant ones as they occur in workspace positions for which also a non-singular joint space solution exists. These so-called *inner singularities* (i.e. those occurring not at the workspace boundaries) have received much attention in recent research as a result of the growing interest in redundant manipulators. In this paper, an 8-degree-of-freedom (DOF) RTR^6 type manipulator is taken as an example, for which the systematic a priori determination of singularity manifolds is explained, with special emphasis on properties arising from the arm's kinematic redundancy. Furthermore, an application of these results is proposed in a local (resolved-motion) planning framework which also allows on-line detection and handling of singularities.

2. Previous Work

As a starting point for the definition of singularities, the differential kinematic model [6, 2]

$$\dot{\mathbf{x}} = \mathbf{J}(\mathbf{q})\dot{\mathbf{q}}; \qquad \mathbf{J} = \left[\begin{array}{cccc} \mathbf{d}_0 & \mathbf{d}_1 & \cdots & \mathbf{d}_{r-1} \\ \mathbf{t}_0 & \mathbf{t}_1 & \cdots & \mathbf{t}_{r-1} \end{array} \right] \tag{1}$$

of the manipulator is used, where $\dot{\mathbf{x}}$ is the end point velocity, $\dot{\mathbf{q}}$ is the vector of joint velocities and $\mathbf{J}(\mathbf{q})$ is the Jacobian matrix for the current configuration $\mathbf{q}$. Given an n-dimensional workspace and a robot with m kinematic DOF, $\dot{\mathbf{x}}$ is an $n \times 1$ column vector, $\dot{\mathbf{q}}$ is an $m \times 1$ column vector and $\mathbf{J}$ is an $n \times m$ matrix. In the non-redundant case, $n = m$; whereas for redundant DOF, $n < m$. Each column of $\mathbf{J}$ describes the contribution of the corresponding joint to the end point motion; $\mathbf{d}_i$ is the effect of joint q_i on the end point's linear velocity, and $\mathbf{t}_i$ is its counterpart for the angular velocity. The manipulator's motion reserve is then defined by the *manipulability ellipsoid*, as introduced by YOSHIKAWA [11]. To obtain the latter, a unit sphere (or an ellipsoid) is drawn around the origin of the joint velocities' coordinate system. Then $\mathbf{J}$ is used to map the joint space sphere onto an ellipsoid in the workspace, whose shape then shows the amount of motion reserve in a given direction of the workspace. In a singular configuration, a rank loss is encountered in $\mathbf{J}$

$$\mathrm{rank}\,(\mathbf{J}(\mathbf{q})) < n, \tag{2}$$

(where n is the workspace dimensionality) which corresponds to a fully flattened ellipsoid and, thus, the exhaustion of the motion reserve in at least one direction. Using the volume of the manipulability ellipsoid, also a scalar manipulability measure S can be defined. According to this measure, a singularity occurs if

$$S := \sqrt{\det\left(\mathbf{J}\mathbf{J}^T\right)} = 0, \tag{3}$$

which is obviously an equivalent statement to (2). Using either one of the above definitions (2,3), one could take the symbolic form of the robot's Jacobian matrix **J** and determine the manifolds for which the above conditions occur. As a result, a first-order logical statement is obtained which can be evaluated for a given configuration to check whether a singularity occurs. This task can be broken down according to the usual *arm and wrist* (linear and angular velocity) concept, as shown by TOURASSIS et al. [10], or a general *mid-frame* decomposition can be made, as proposed by DOTY [3]; the latter also applying the same method for both redundant and non-redundant manipulators.

Singularity detection during motion planning or execution can be performed either by checking with the previously obtained singularity manifolds or examining the numerical properties of $\mathbf{J}(\mathbf{q})$. Upon detecting a singular configuration (or its proximity), an 'exception handling' procedure can be triggered. When a robot drives through a singular configuration, the inverse kinematic solution (a $\dot{\mathbf{q}}$ to a prescribed $\dot{\mathbf{x}}$) would deliver unacceptably high joint space velocities; therefore, the primary goal of all singularity handling methods is to guarantee joint velocities below a given limit at the cost of a local change in the workspace motion of the robot's end point. Some of these techniques modify the numeric properties of **J** with the trade-off of an imperfect $\dot{\mathbf{x}}$, such as the *damped least-squares* approach, as shown by DE WIT et al. [2] or FORET et al. [4], while others (as NENCHEV et al. [1] or LLOYD et al. [8]) alter the time scales of one or more components in the joint space; either to take a virtual bypass around the singularity (again, at the cost of imprecise workspace motion), or to maintain acceptable joint velocities while locally slowing down the end point motion to zero.

3. Determining Singularity Manifolds of an 8-DOF Arm

In this example, the singularity manifolds are determined using the decomposition principle. The procedure is demonstrated on a specific 8-DOF arm constructed for Siemens Corporate Technology in Munich, Germany, for the use in a mobile manipulator for service robotic experiments. The manipulator resembles a human arm in its structure; therefore, the joints also have a name corresponding to their placement and function, as shown in *Fig. 1*.

It is known that manipulators whose last three axes meet in one point (as the one dealt with in this paper), can be decomposed into a positioning and a rotating part [6]. While this principle is mainly used to break up the *inverse kinematic* problem into two smaller parts, it can be carried on to the *differential kinematic* level, i.e. to the relation of linear, angular and joint velocities as well. Therefore, it is generally assumed that the manipulator in question is to guarantee the prescribed angular velocity of the end point with its last three segments (LA, WT and WP in our case), while the rest of the robot is responsible for the correct linear velocity. A further consequence of this decomposition is that a full Cartesian motion command (both linear and angular velocity prescribed at the end point) would imply a

Joint #	Type	Name	
q_1	R	TR;	Tower Rotate
q_2	T	TL;	Tower Lift
q_3	R	SH;	Shoulder
q_4	R	UA;	Upper Arm
q_5	R	EL;	Elbow
q_6	R	LA;	Lower Arm
q_7	R	WT;	Wrist Tilt
q_8	R	WP;	Wrist Pan
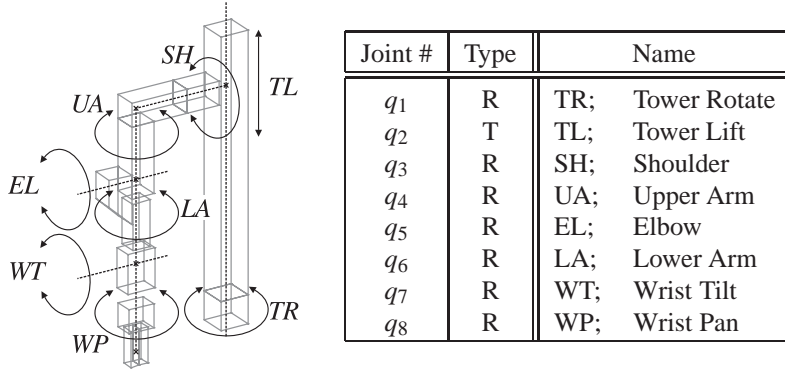
Fig. 1. Joint names of the 8-DOF manipulator

pure linear motion task three joints further 'upward.' This already hints at a possible principle of our singularity search: first, all cases should be found where this remaining linear motion task cannot be carried out (since then, the last three joints, all applied to ensure the prescribed angular velocity, cannot add further linear motion reserve); thereafter, the case of a singular wrist (i. e. when the last three joints cannot perform the desired rotatory motion alone) should be examined.

To facilitate further visualization, let us denote some significant points and directions on the manipulator, as shown in *Fig. 2*. Here, point O is the intersection of the robot's TR and SH axes, point A is the intersection of the axes SH and UA, B is the intersection of UA and EL (or EL and LA as well), C is the intersection of LA and WT (or WT and WP), and finally, E is the manipulator's end point. Drawing a cylindrical coordinate system around the TR or TL axis (these are, of course, collinear), one could mark three directions of linear motion: an axial (parallel to the tower axis), a radial (passing perpendicularly through the tower axis) and a tangential direction. Having set up these naming conventions, now the two cases of singularity search are examined.

Case 1: Wrist Is Nonsingular

As mentioned before, in this case, one can regard a full motion command for E as a pure velocity command for the wrist center, i. e. C. A singular configuration thus occurs if the motion reserve of C with respect to linear velocity is exhausted. Recalling the differential kinematic equation (1), this would mean that the first five columns of the 6×8 Jacobian matrix $\mathbf{J}$ could not 'serve' the first three components of $\dot{\mathbf{x}}$, i. e. the submatrix $[\mathbf{d}_0 \ldots \mathbf{d}_4]$ is singular. In this case, the remaining three columns of $\mathbf{J}$ are not eligible for help, regardless of the 'wrist' being nonsingular or singular, since they are fully assigned to the remaining three dimensions of Cartesian workspace (i. e. orientation or angular velocity).
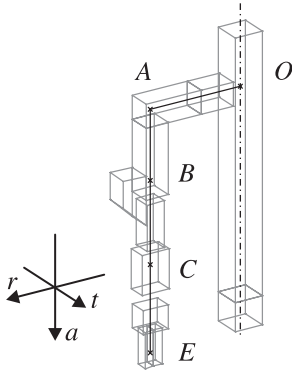
Fig. 2. Important points and motion directions
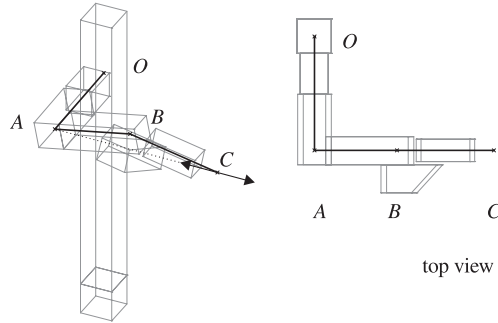
Fig. 3. Points O, A and C in a radial/tangential plane

To begin with the search for critical configurations, let us first look at the contribution of TR and TL. It can be seen that (omitting joint limits) TR can always rotate and TL can always shift along the same axis through O, constantly ensuring a tangential and an axial motion reserve (see *Fig. 2*), respectively. Therefore, the only deficiency in motion reserve can occur in the radial direction. The invariance of TR and TL would furthermore suggest that a motion deficiency can only be caused by SH, UA and EL, leaving thus only three joints to be examined.

First, let us take SH into consideration. If only the shoulder joint were to move C, the wrist center would move in a circle whose plane is perpendicular to $\overline{OA}$. The radial motion reserve would be exhausted when either O, A and C are in the same radial/axial plane or when O, A and C are in the same radial/tangential plane. It can be shown that also B has to be in the same plane, for which the following two setups should be examined.

If O, A and C are in the same radial/tangential plane, a radial motion can be still introduced by 'flattening' the $\widehat{ABC}$ triangle as shown in *Fig. 3* (note that the radial direction is given by $\overline{OC}$), or, as shown in *Fig. 4*, by applying the UA joint. Are O, A and C in the same radial/axial plane, as in *Fig. 4*, flattening the triangle would give an axial motion which is of little use, however, UA does still introduce a radial reserve.

This proves that B also has to be in the same plane as O, A and C if a singular configuration for the linear motion of C is sought. Therefore, only two eligible configuration pairs can be selected for the shoulder joint:

- SH $\in \{0, \pm\pi\}$
- SH $= \pm^{\pi}/_{2}$

Shoulder is 'vertical' – If SH $\in \{0, \pm\pi\}$, all the four above mentioned points are
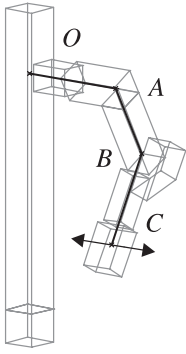
Fig. 4. O, A, C in a radial/axial plane
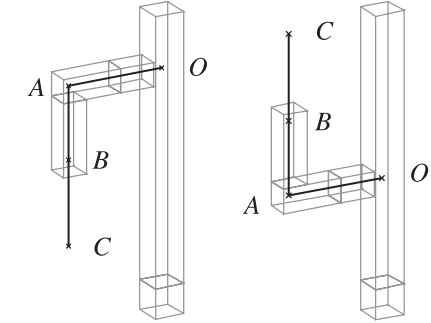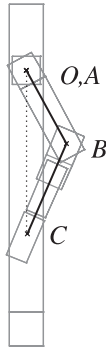
Fig. 5. 'Vertical' shoulder configurations: SH = 0 and SH = $\pm\pi$

in the radial/axial plane (as in *Fig. 5*). Now, let us examine three different cases for UA:

- If UA is in an 'intermediate' configuration, two cases may occur:
    - If EL $\notin \{0, \pm\pi\}$, at least UA can introduce a radial reserve.
    - If EL $\in \{0, \pm\pi\}$, at least EL gives radial reserve.
- If UA $= \pm^\pi/_2$, EL can move C only within the radial/axial plane. Here, EL can contribute to radial motion as long as EL $\neq \pm^\pi/_2$. Does the latter occur, no other joint can give further radial motion reserve for C, this is therefore a singular configuration (*Fig. 6*).
- Is UA $\in \{0, \pm\pi\}$, EL can move C in the axial/tangential plane through B. The only case here in which C is in the same plane as the other points, is EL $\in \{0, \pm\pi\}$ (*Fig. 7*), when none of the joints is able to move C radially, thus giving the second set of singular configurations.

Shoulder is 'horizontal' – If SH $\in \{0, \pm\pi\}$, all the four above mentioned points are in the radial/tangential plane. Again, three different cases have to be examined for UA:

- If UA is in an 'intermediate' configuration, two cases may occur, both similar to those with a "vertical" shoulder alignment:
    - If EL $\notin \{0, \pm\pi\}$, at least UA can introduce a radial reserve.
    - If EL $\in \{0, \pm\pi\}$, at least EL gives radial reserve.
- Is UA $\in \{0, \pm\pi\}$, then only EL $\in \{0, \pm\pi\}$ can keep C in the same radial/axial plane as all the other points, as shown in *Fig. 8*. For any other setting of EL, UA could have added a radial motion reserve; for EL $\in \{0, \pm\pi\}$, however, not even EL does; therefore, we have found another set of singular configurations.
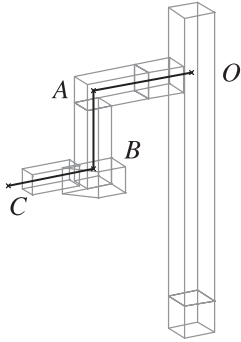
Fig. 6. Singular configuration SH $= 0$, UA $= {}^\pi/_2$, EL $= -{}^\pi/_2$
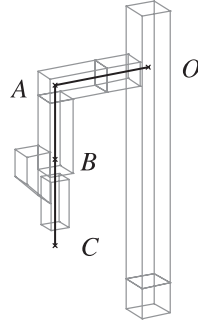
Fig. 7. Singular configuration SH $= 0$, UA $= 0$, EL $= 0$
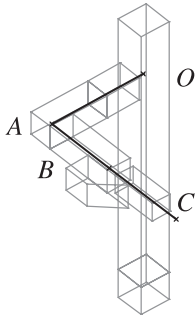
Fig. 8. Singular configuration SH $= {}^\pi/_2$, UA $= 0$, EL $= 0$
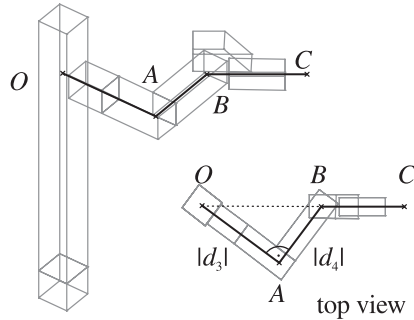
Fig. 9. Singular configuration SH $= {}^\pi/_2$, UA $= {}^\pi/_2$, EL $= -\tan^{-1}|{}^{d_3}/_{d_4}|$

- If UA $= \pm{}^\pi/_2$, all relevant points lie in the same radial/tangential plane where EL moves C in a circle around B. It is easy to see that EL cannot add radial motion reserve if O, B and C are on the same line, which would mean a pair of configuration sets for each value of UA. This would mean EL $= -\tan^{-1}|\frac{d_3}{d_4}| \pm \{{}^0_\pi\}$ for UA $= {}^\pi/_2$ (as in *Fig. 9*) and EL $= \tan^{-1}|\frac{d_3}{d_4}| \pm \{{}^0_\pi\}$ for UA $= -{}^\pi/_2$. Thus, this is the last group of singular configurations which are related to motion reserve deficiency at the wrist center C.

Summarizing these cases, four sets of configurations can be selected where singularity occurs due to the exhaustion of radial motion reserve for C (cases L1–L4 in *Tab. 1*).

Case 2: Wrist Is Singular

The last three joints of the robot (LA, WT and WP) form an "Euler wrist" which is responsible for setting the orientation at the end point E. If WT is in an "intermediate" setting, the three axes do not lie in one plane and therefore, they can realize any rotational velocity at E. The problem occurs if WT $\in \{0, \pm\pi\}$, since then, LA and WP have a common axis whereby one dimension of rotational reserve is lost in the wrist. In the differential kinematic equation (1), this would mean that the submatrix $[\mathbf{t}_5 \ldots \mathbf{t}_7]$ is singular. This alone, however, does not necessarily imply a singular configuration for the entire robot. Since our 8-DOF arm is kinematically redundant, we may find a column $\mathbf{t}_i$ in $[\mathbf{t}_0 \ldots \mathbf{t}_4]$ which makes up a full-rank matrix together with $[\mathbf{t}_5 \ldots \mathbf{t}_7]$ while the remaining part of the robot can still complete the linear motion task, i. e. $[\mathbf{d}_0 \ldots \mathbf{d}_{i-1} \, \mathbf{d}_{i+1} \ldots \mathbf{d}_4]$ still has full rank. This replacement would suit any *revolute* joint among {TR, SH, UA, EL} which has the following two properties:

- the axis of the joint is not parallel to the plane of LA/WP and WT,
- the additional motion of C resulting from the use of the joint concerned can be compensated by the rest of the first five joints (including TL when needed).

If both statements hold for a given joint, it will be called a *'replacement joint'*. A *'candidate replacement joint'* would be one for which the first statement holds while the second may or may not be true. Obviously, a singular wrist means singularity for the entire arm if no suitable replacement joint can be found. In a formal expression, this would mean:

$$(\text{WT} \in \{0, \pm\pi\}) \wedge ((\text{no repl. exists}) \vee (C \text{ has no radial reserve}))$$
$$\longrightarrow (\det(\mathbf{J}\mathbf{J}^T) = 0). \tag{4}$$

It must be noted that the exhaustion of the radial motion reserve at C is already covered by L1–L4; therefore, new singularity manifolds will only be added if no replacement joint is found in a given case. To set up a search strategy, let us first see when it is possible at all that no replacement joint can be found. Now, let us examine the replacement possibilities by the number of replacement candidates.

Let us first assume that all four revolute joints are replacement candidates. Picking now one joint for replacement, the compensation of C's motion will have to be accomplished by the remaining three revolute joints plus TL. The worst case occurs if the selected replacement candidate adds a motion to C that cannot be compensated by the rest. Is this the case, there are still three other revolute joints left as candidates. If we then again pick one whose motion cannot be compensated, we have two revolute joints plus TL which necessarily *must* solve the replacement problem, because the still eligible candidate joints add the same reserve to the linear motion as TL. (The only joint that would not add further motion to C at all would be UA for EL $\in \{0, \pm\pi\}$, which would rule UA out as a candidate anyway, due to the coaxiality to LA/WP. TR is kept from such a situation because of arm

length parameters, neither would SH and EL show this property due to similar reasons.) Therefore, if all revolute joints are replacement candidates, no singular configuration will occur – unless any of L1–L4 is encountered.

If one of the first four revolute joints is not a valid candidate, we can choose from three other candidates. First, let us assume that the non-candidate adds a (nonzero) motion reserve which cannot be used for the compensation of the prospective replacement joints. In this case, two Cartesian dimensions of motion reserve remain for the rest. As for TL, the worst case would be that its motion contribution would be that of the non-candidate joint. Then, picking one candidate for replacement would leave two others for compensation. If the joint initially chosen cannot be compensated, the remaining two would still give a valid solution, since then, they would have to share the same Cartesian degree of freedom. Now, let us consider the case when the non-candidate joint would not add any motion reserve. In this case, picking a candidate with no possibility of compensation would leave two other candidates and two Cartesian dimensions of motion reserve to be provided at C. If, again, one candidate is picked whose motion contribution cannot be compensated, only one revolute joint remains which then has to share the same Cartesian dimension of resultant motion as TL. Again, we would have no possibility of a singular configuration, save for the restricted motion reserve cases of L1–L4.

The case of two non-candidate joints is, however, different. The worst case would be that these non-eligible joints could not be used for compensating motion either, so that we have two revolute joints plus TL for the entire compensating task. If the two non-candidate joints added altogether one dimension of motion reserve at C which cannot be used for compensation, we would have two candidates left which would have to serve two Cartesian dimensions. If the contribution of TL is in the same direction as that of the non-candidate joints, two joints would remain for the two Cartesian dimensions, making a replacement impossible. Therefore, there must be at least two non-candidate joints among {TR, SH, UA, EL} to cause a singular configuration other than L1–L4. Based on this conclusion, the following search strategy can be formed:

1. Determine the configurations in which a given joint is not an eligible replacement candidate.
2. Form all cases in which two or more of the first four revolute joints cannot be used for replacement.
3. Examine all cases for suitable motion compensation and motion reserve at C and mark the singular configurations found.
4. Rule out configurations or manifolds which are already covered by others (including L1–L4).

The first step of the search returns – putting 'symmetrical' cases into the same group – 15 independent configuration manifolds, combining to 47 different sets which comply with step 2. Since in these manifolds, at most two relevant joint values are unknown, their examination for singularity is not too demanding. Thus,

Table 1. Singular configuration manifolds

Name	TR	TL	SH	UA	EL	LA	WT	WP
L1			$\left\{{0\atop\pm\pi}\right\}$	$\pm\pi/2$	$\pm\pi/2$			
L2			$\left\{{0\atop\pm\pi}\right\}$	$\left\{{0\atop\pm\pi}\right\}$	$\left\{{0\atop\pm\pi}\right\}$			
L3			$\pm\pi/2$	$\left\{{0\atop\pm\pi}\right\}$	$\left\{{0\atop\pm\pi}\right\}$			
L4			$\pm\pi/2$	$+\pi/2$ $-\pi/2$	$-\tan^{-1}\left|\frac{d_3}{d_4}\right|\pm\left\{{0\atop\pi}\right\}$ $+\tan^{-1}\left|\frac{d_3}{d_4}\right|\pm\left\{{0\atop\pi}\right\}$			
A1				$\left\{{0\atop\pm\pi}\right\}$	$\left\{{0\atop\pm\pi}\right\}$	$\left\{{0\atop\pm\pi}\right\}$	$\left\{{0\atop\pm\pi}\right\}$	
A2			$\left\{{0\atop\pm\pi}\right\}$		$\pm\pi/2$	$\left\{{0\atop\pm\pi}\right\}$	$\left\{{0\atop\pm\pi}\right\}$	
A3			$\left\{{0\atop\pm\pi}\right\}$	$\pm\pi/2$		$\pm\pi/2$	$\left\{{0\atop\pm\pi}\right\}$	
A4			$\pm\pi/2$	$\pm\pi/2$		$\pm\pi/2$	$\left\{{0\atop\pm\pi}\right\}$	
A5			$\left\{{0\atop\pm\pi}\right\}$	$\rightarrow$LA	0 $\pm\pi$	UA+LA $\in$ $\left\{{0\atop\pm\pi}\right\}$ UA−LA $\in$ $\left\{{0\atop\pm\pi}\right\}$	$\left\{{0\atop\pm\pi}\right\}$	
A6			$\pm\pi/2$	$\rightarrow$LA	0 $\pm\pi$	UA+LA $\in$ $\left\{{0\atop\pm\pi}\right\}$ UA−LA $\in$ $\left\{{0\atop\pm\pi}\right\}$	$\left\{{0\atop\pm\pi}\right\}$	

performing steps 3 and 4 returns six more sets of singular configurations (cases A1–A6 in *Table 1*)

4. Application in Local Motion Planning

Since kinematic singularities impose limits on the robot's motion capabilities, their knowledge may be essential for the successful execution of workspace velocity commands. If a global planning approach is taken, singularity manifolds are present as virtual obstacles constraining the *configuration space* and a suitable planner can guide the robot around them. Local planning methods, however, cannot use an explicit topological representation, and thus, other means must be chosen to cope with singularities. In this section, two suggestions for such local approaches are proposed.

Virtual Forces and Joint Space Constraints

Though singularity manifolds cannot be used in local planning in the topological way of global methods, they can be locally present, e. g. through the gradient of an objective function. For kinematically redundant manipulators, it is possible to apply such a gradient as a secondary motion preference while the end point of the robot executes a prescribed workspace velocity command. In this case, the singularity manifolds can exert a *virtual force* which attempts to push the manipulator's configuration away from the critical area of configuration space. The most widespread method used to apply such a secondary motion criterion (the primary requirement being a prescribed end point motion in the workspace) is the *gradient projection method*, introduced by LIEGEOIS [7], which solves the inverse differential kinematic problem of redundant robots by the following equation:

$$\dot{\mathbf{q}} = \dot{\mathbf{q}}_p + \dot{\mathbf{q}}_h = \mathbf{J}^+\dot{\mathbf{x}} + \alpha\mathbf{N}_{proj}\mathbf{h}, \tag{5}$$

where $\dot{\mathbf{q}}_p$ is the particular part ensuring the end point motion with a minimum-norm joint velocity, while $\dot{\mathbf{q}}_h$ is the homogeneous term, i. e. the projection of a joint velocity preference $\mathbf{h} = \partial Q(\mathbf{q})/\partial\mathbf{q}$, in our case the gradient of a virtual potential function $Q(\mathbf{q})$, into the null space of $\mathbf{J}$ with a projection matrix $\mathbf{N}_{proj}$ (and the scaling factor α). While gradient projection is simple and computationally not demanding, it is unable to *guarantee* the value of selected joint velocity components or their linear combination and, thus, is not suited to meet *hard* motion requirements, as would be needed for collision avoidance cases or joint limits.

This shortcoming can be mended by the FSP (Full Space Parameterization) of PIN et al. [9], and the closely related but numerically more robust PNS (Parameterization through Null Space) suggested by the author of this paper [5] which solve the inverse differential kinematic problem by an optionally constrained closed-formula optimization. To find a suitable $\dot{\mathbf{q}}$ for a prescribed $\dot{\mathbf{x}}$, both methods first find a solution space in form of base vectors. From these, a weight vector $\mathbf{t}$ can create a linear combination which optimizes a quadratic criterion of the form

$$\min_{\dot{\mathbf{q}}} \frac{1}{2} \|\mathbf{B}\dot{\mathbf{q}} - \mathbf{z}_r\|^2 \tag{6}$$

with optional constraints of the linear equality form

$$\boldsymbol{\beta}^T\mathbf{t} - \mathbf{e} = \mathbf{0}, \tag{7}$$

where $\mathbf{B}$ is a weighting (or preference transformation) matrix, $\mathbf{z}_r$ is a motion preference, which would be equivalent to $\alpha\mathbf{Bh}$ using the naming convention of (5), while $\boldsymbol{\beta}$ is a constraint coefficient matrix and $\mathbf{e}$ is a vector with 1.0 for all elements. In [5], a method was proposed to integrate the abilities of criteria and constraints into a local motion planning framework. In this scheme, the arm is kept near a preferred configuration using the motion criterion (6). For $\mathbf{B}$, a full-rank diagonal matrix is used whose diagonal elements can be chosen according to the weighting

preferences of a given task, while $\mathbf{z}_r$ is combined from the outputs of an array of saturated P-controllers. For the latter, the component-wise difference of the actual and the desired configuration is taken for a control error. While this setup, as shown in *Fig. 10*, resembles closed-loop control, the manipulator will not actually reach the preferred configuration if this is not possible with the given workspace motion command. It should be also noted that with the application of simple P-type controllers, this configuration control still represents a gradient-based approach.
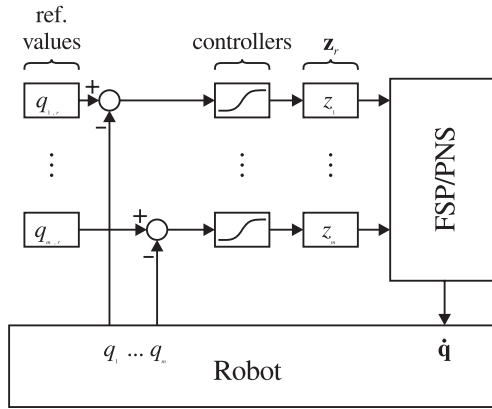
Fig. 10. Configuration control with criteria in FSP/PNS

The constraints were applied to meet a 'hard' requirement: the gradual deceleration of a given joint before reaching its joint limit. Here, the range of each joint is padded by a safety zone. First, all joint velocities are checked for the following condition:

$$\left((\dot{q}_i < 0) \wedge (q_i < q_{i,l})\right) \vee \left((\dot{q}_i > 0) \wedge (q_i > q_{i,h})\right), \tag{8}$$

where $q_{i,l}$ denotes the beginning of the safety zone around the lower limit of joint i; similarly, $q_{i,h}$ applies to the upper safety zone of the same joint. Does (8) hold for a given joint q_i and its velocity $\dot{q}_i$ (i. e. q_i is moving towards the joint limit within its safety zone), its previously calculated unconstrained velocity $\dot{q}_{,unc}$ is scaled down with a quadratic function, and this $\dot{q}_{i,cons} := s_i(q_i)\dot{q}_{i,unc}$ is then ensured by an additional optimization constraint. An example of the quadratic scaling function $s_i(q_i)$ is shown in *Fig. 12*, while the deceleration effect of the applied constraint is shown in *Fig. 13* for a given joint of the robot (the gray background denotes the safety zone in both figures). It must be noted, however, that the maximal number of applicable constraints is limited by the dimensionality of the optimization space, i. e. by the number of redundant DOF. Would more joint limits be approached than
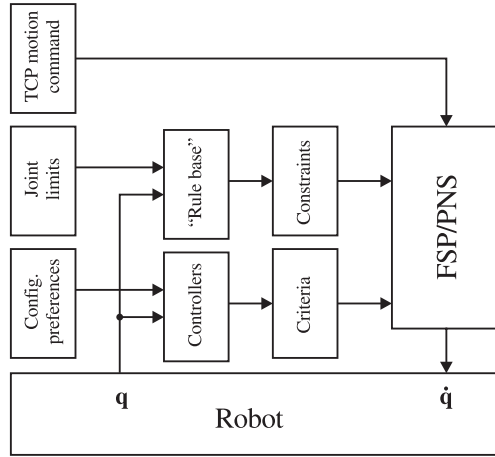
Fig. 11. Complete scheme of local motion planning using FSP/PNS

the maximal allowable number, it would be, of course, impossible to execute the prescribed end point motion due to dimensionality problems.
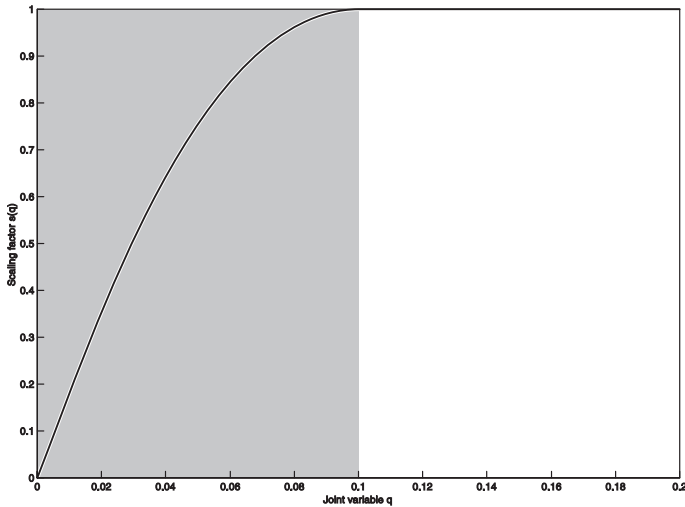
Fig. 12. Quadratic scaling function $s_i(q_i)$ for $q_{i,l} = 0.1$ and a joint limit at $q = 0$

The configuration preference and joint limit handling functionalities were integrated into one algorithm as shown in *Fig. 11*. This scheme, though originally not designed for singularity avoidance, can offer two main opportunities of singularity handling.
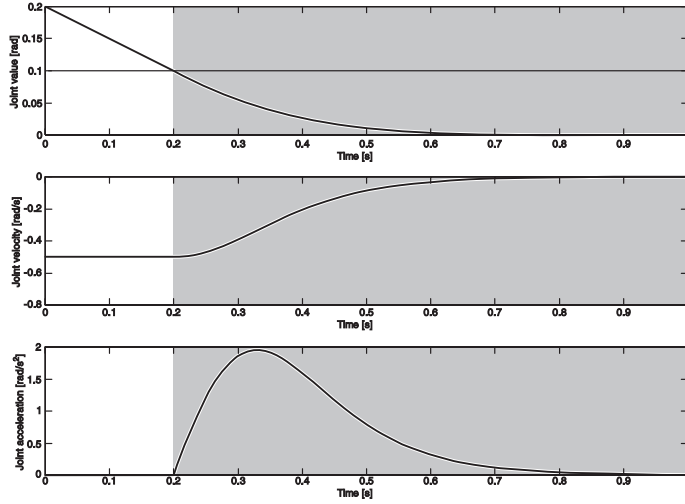
Fig. 13. Joint value, velocity and acceleration for a case of joint limit handling

First, one can set *virtual joint limits* so that the partition of the configuration space enclosed is free of singularities. These new limits can be protected by a safety zone and handled by the application of constraints as described before. While this does not even require a different principle in the application of the numeric method, the motion capabilities of the robot would be considerably limited and therefore, only the protection of critical yet confined motion tasks could be considered.

The other approach is more elaborate and takes a *subspace* of the entire configuration space into consideration. Observing *Table 1*, it can be seen that every singularity manifold shrinks to a point or a finite set of points if only the appropriate components of **q** are taken. In the case of e. g. manifold L1, the adequate subspace would be given by the components $\mathcal{S} := \{SH,UA,EL\}$ and the corresponding $\mathbf{q}_{\mathcal{S}}$ would be comprised of the adequate elements of **q**. (If the linear combination of several joints is involved, as in A5 and A6, a transformation can be found which maps this onto one given dimension.) In this subspace, a Euclidean distance from a given singularity could be calculated by

$$d := \sqrt{\sum_{i \in S} (q_{i,sing} - q_i)^2}, \tag{9}$$

where $q_{i,sing}$ is the value of q_i for the singularity. Also a unit-norm vector can be defined to describe the difference of $\mathbf{q}_{\mathcal{S}}$ and the singularity:

$$\mathbf{d}_{\mathcal{S}} := \frac{\mathbf{q}_{\mathcal{S},sing} - \mathbf{q}_{\mathcal{S}}}{d}; \quad ||\mathbf{d}_{\mathcal{S}}|| = 1, \tag{10}$$

where $\mathbf{q}_{\mathcal{S},sing}$ is the specific instance of joint values for the singularity, and $\mathbf{q}_{\mathcal{S}}$ contains the components of the current configuration which are in the subspace.

Now, given d and $\mathbf{d}_{\mathcal{S}}$, two approaches may be taken. First, one could make up a virtual force in the radially symmetric form $\mathbf{f}_{\mathcal{S}} := f(d)\mathbf{d}_{\mathcal{S}}$ which, applied through the criterion's motion preference $\mathbf{z}_r$, attempts to repel the robot from the singularity. Second, a safety (hyper)sphere may be drawn around the singularity and analogously to (8), the following condition can be checked:

$$(d < d_{safe}) \wedge (\mathbf{d}_{\mathcal{S}}^T \dot{\mathbf{q}}_{\mathcal{S}} > 0), \tag{11}$$

where d_{safe} is the radius of the safety zone. If this zone is entered and the robot moves towards the singularity, (11) becomes true and a gradual deceleration can be effected with constraints, similarly to that shown in *Figs. 12* and *13*, except that here, full stop in radial direction should be reached *before* encountering the singularity, at a minimal "circumvention distance" $0 < d_{circ} < d_{safe}$. Since in this case, only the radial direction towards the singularity is relevant, the corresponding constraint should be set for a linear combination of joint velocities, weighted according to the components of $\mathbf{d}_{\mathcal{S}}$. This represents exactly the radial direction and diminishes the reserve of the optimization space only by one dimension.

The method outlined in *Fig. 11* was implemented for the 8-DOF arm described earlier in this paper, incorporating the configuration control according to a preference and the joint limit handling, both ensuring continuous joint acceleration through time. The algorithm was tested in simulations using the differential kinematic model, and on the robot itself as well, within the framework of sensor-guided manipulation tasks. Simulations for the singularity avoidance extension of the algorithm are now in progress, and tests on the physical robot are in preparation.

Numerical Singularity Detection and Handling

While it is possible to check the arm's current configuration with the previously obtained singularity map (either in the form of rules or as virtual forces), it is also possible to detect singularities through the numerical examination of the robot's Jacobian matrix $\mathbf{J}$. The above mentioned PNS method offers an easy way of accessing such kinematic properties, since in the first step of the procedure (as outlined in *Fig. 14*) is the singular value decomposition (SVD) of $\mathbf{J}$, which delivers the nonnegative singular values $\{\sigma_i\}$ of $\mathbf{J}$ in a diagonal matrix. The $\{\sigma_n\} \subset \{\sigma_i\}$ belonging to the null space of $\mathbf{J}$ are zero, while the others (let them denote $\{\sigma_a\}$) are positive, if the arm is not singular. Approaching a singularity, one or more of the $\{\sigma_a\}$ diminishes rapidly and exactly in the singularity, they become zero, just as the scalar measure of motion reserve, $\prod_a \sigma_a$, does.

Since the Moore–Penrose pseudoinverse $\mathbf{J}^+$, calculated with the reciprocal $\{\sigma_a\}$, is used to obtain the inverse differential kinematic solution, it is clear that singularities impose a serious hindrance, and even their vicinity is marked by unacceptably high joint velocities in the minimum-norm solution $\mathbf{J}^+\dot{\mathbf{x}}$. To avoid this,
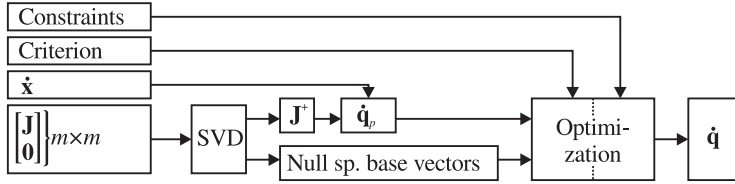
Fig. 14. Schematic structure of the PNS method

a "symptomatic" treatment of singularities can be applied, as proposed in [5]. First, the singular values $\{\sigma_a\}$ are examined for the following condition:

$$\sigma_a < 2\sigma_{crit}; \quad \sigma_{crit} := \sigma_{max}\varepsilon, \tag{12}$$

where σ_{max} is the maximal singular value among $\{\sigma_a\}$ and ε is a small threshold value, typically in the 10^{-3} range. Should a σ_a drop below the critical value, a quadratic function is used to "prop up" this σ_a, i.e. it is kept above a minimal value:

$$\sigma_{a,mod} := \frac{\sigma_a^2}{4\sigma_{crit}} + \sigma_{crit}, \tag{13}$$

after which the modified singular value $\sigma_{a,mod}$ is used in the calculation of $\mathbf{J}^+$. This results in acceptable joint velocities obtained by $\mathbf{J}^+\dot{\mathbf{x}}$ (and continuous joint acceleration as well); at the cost of inaccuracies in the resulting end-point motion. This trade-off, closely related to the *damped least squares* technique [2], allows the robot to pass through singularities. The optimization task in later parts of the PNS method does not suffer numerical deterioration (unlike FSP), since in PNS, the optimization space is set up using the orthonormal base vectors of $\mathbf{J}$'s null space as obtained by the singular value decomposition, where singular configurations cause neither scaling problems nor rank loss.

The singularity detection and handling method presented above was implemented and successfully tested as a part of the local motion planning functionalities for the 8-DOF arm mentioned in this paper.

5. Conclusion

In this paper, a systematic singularity search technique for kinematically redundant manipulators was presented, using the example of an existing 8-DOF manipulator. The approach uses the decomposition principle of serial manipulators to appoint two classes of singular configurations; the first resulting from the singularity of the "truncated" kinematics (exhaustion of the linear motion reserve) and the second implied by a singular wrist (a deteriorated angular motion reserve of the end point). Furthermore, the application of the so derived singularity map was proposed for

local motion planning. Also, a method for the on-line detection and local treatment of encountered singularities was shown, which was implemented and successfully tested on the above mentioned 8-DOF manipulator.

Acknowledgement

References

[1] NENCHEV, N. – TSUMAKI, D. Y. – UCHIYAMA, M., Singularity-Consistent Parameterization of Robot Motion and Control, *The International Journal of Robotics Research*, **19** (2) February (2002), pp. 159–182.

[2] DE WIT, C. C. – SICILIANO, B. – BASTIN, G., (editors). *Theory of Robot Control*, Springer-Verlag London Ltd., 1996.

[3] DOTY, K. L., Jacobians and Singularities, Technical Report MIL050992kld, Machine Intelligence Laboratory, University of Florida, 1992.

[4] FORET, J. – XIE, M. – FONTAINE, J. G., Bordered Matrix for Singularity Robust Inverse Kinematics: A Methodological Aspect, In *Proceedings of the 2000 IEEE International Conference on Robotics and Automation*, San Francisco, CA, pp. 3013–3019, April 2000.

[5] KEMÉNY, ZS., Parameterization Through Null Space – A New Redundancy Resolution Method for Differential Kinematic Problems in Comparison to Other Methods, In *Proceedings of the 2002 IEEE International Conference on Intelligent Engineering Systems INES'2002*, Opatija, Croatia, pp. 161–166, May 2002.

[6] LANTOS, B., *Robotok irányítása*, Akadémiai Kiadó, Budapest, 1991.

[7] LIEGEOIS, A., Automatic Supervisory Control of Configurations and Behavior of Multibody Mechanisms, *IEEE Transactions on Systems, Man and Cybernetics*, SMC-7(12) December (1977), pp. 868–871.

[8] LLOYD, J. E. – HAYWARD, V., Singularity-Robust Trajectory Generation, *The International Journal of Robotics Research*, **20** (1) January (2001), pp. 38–56.

[9] PIN, F. G. – TULLOCH, F. A., Resolving Kinematic Redundancy with Constraints Using the FSP (Full Space Parameterization) Approach, In *Proceedings of the 1996 IEEE International Conference on Robotics and Automation*, pp. 468–473, April 1996.

[10] TOURASSIS, V. D. – ANG, M. H. JR., Identification and Analysis of Robot Manipulator Singularities, *The International Journal of Robotics Research*, **11** (3) (1992), pp. 248–259.

[11] YOSHIKAWA, T., Manipulability of Robotic Mechanisms, *The International Journal of Robotics Research*, **4**(2) (1985), pp. 3–9.